Co$_9$S$_8$ Nanotubes as an Efficient Catalyst for Hydrogen Evolution Reaction in Alkaline Electrolyte

Lihuang Jin, Cuncai Lv, Jie Wang, Han Xia, Yaoxing Zhao, Zhipeng Huang[*]

Scientific Research Academy, Jiangsu University, Zhenjiang, China
Email: [*]zphuang@ujs.edu.cn

Abstract

Cobalt sulfide (Co$_9$S$_8$) nanotubes were found to be an electrocatalyst for the hydrogen evolution reaction under alkaline condition. An electrode comprising of Co$_9$S$_8$ nanotubes on a glass carbon electrode (GCE) (mass loading: 0.855 mg·cm^{-2}) produced a cathodic current density of 20 mA·cm^{-2} at an overpotential of 320 mV. The Co$_9$S$_8$/GCE electrode was stable over 20,000 s during potentiostatic electrolysis. Minor degradation of reduction current after 4000 cyclic voltammetric sweeps suggests the long-term viability under operating conditions. The faradaic efficiency of Co$_9$S$_8$ nanotubes is nearly 100% during the electrolysis of water.

Keywords

Cobalt Sulfide Nanotubes, Electrocatalyst, Hydrogen Evolution Reaction, Alkaline Electrolyte

1. Introduction

Hydrogen has been considered as a clean and efficient fuel in the transition from the current hydrocarbon economy because of the climate change and the shortage of fossil fuels [1]-[3]. Though the hydrogen evolution reaction (HER) can be effectively facilitated by Pt-group metals, the high cost and scarcity of Pt-group metals make the widespread application of these catalysts difficult. The exploitation of efficient HER catalysts among low cost and abundant compound is therefore desirable [4]. Successful examples include MoS$_2$ [4]-[7], WS$_2$ [8] [9], WS$_3$ [9], CoS$_2$ [10], MoSe$_2$ [11] [12], WSe$_2$ [12], CoSe$_2$ [13], MoB [14], Mo$_2$C [15], NiMoN$_x$ [16], Co$_{0.6}$Mo$_{1.4}$N$_2$ [17], MoP [18], Ni$_2$P [19], Ni$_{12}$P$_5$ [20], Co$_2$P [21], and CoP [22].

---

[*]Corresponding author.

Because most electrode materials suffer from corrosion in acidic condition, alkaline water electrolysis is widely adopted in industry [3]. Nowadays, the Co-based materials have attracted considerable attention due to their high activity toward HER and low cost, especially in the aspect of alkaline water electrolysis. In this study, we show that Co_9S_8 nanotubes can work as an earth-abundant electrocatalyst with efficient catalytic activity and excellent stability during HER in basic solution.

2. Experimental

2.1. Materials Synthesis

The method used in the synthesis of $Co(CO_3)_{0.35}Cl_{0.20}(OH)_{1.10}$ nanorods was adopted from those reported in ref [23] [24]. Then, 0.6 mmol of the as-prepared $Co(CO_3)_{0.35}Cl_{0.20}(OH)_{1.10}$ and 0.629 mL of a supersaturated Na_2S aqueous solution were loaded into a Teflon liner (40 mL) with 30 ml distilled water [24]. The liner was sealed in a stainless steel autoclave and maintained at 160˚C for 8 h, then cooled naturally to room temperature. The black precipitates were filtered off, washed with distilled water and ethanol, and then dried at 60˚C.

2.2. Material Characterization

The morphologies were accessed by scanning electron microscopy (SEM, 7001F, JEOL) and transmission electron microscopy (TEM, 2100, JEOL). The X-ray photoelectron spectroscopy (XPS) experiments were carried out on a Physical Electronics PHI 5700 ESCA System. Powder X-ray diffraction (XRD) patterns were collected with a D8 ADVANCE.

The electrochemical measurements were carried out in an 1M KOH aqueous solution with an electrochemical workstation (CHI614D, CH Instrument). A three-electrode configuration was adopted in the measurements, with Co_9S_8 loading on GCE as the working electrode, a graphite rodas the counter electrode and a Mercury/Mercury Oxide electrode (MOE, Hg/HgO) as the reference electrode. The reversible hydrogen evolution potential (RHE) was determined to be −0.879 V vs MOE by the open circuit potential of a clean Pt electrode in the same solution. For the evaluation of HER catalytic activity, Co_9S_8 nanotubes (4 mg) were dispersed in 1 mL of water/ethanol (4/1, V/V) containing 80 μL of Nafion solution (5 wt%). The evaluation of the HER catalytic activity of Co_9S_8 loaded on GCE was carried out by linear sweep voltammetry (5 mV·s^{-1}). The volume of H_2 during potentiostatic electrolysis measurement was monitored by volume displacement in a configuration as shown in ref [21].

3. Results and Discussions

The morphology of Co_9S_8 was examined by SEM. **Figure 1(a)** shows that nanotubes are arranged in a radial fashion. A SEM image with higher magnification (**Figure 1(b)**) shows that the surfaces of the nanotubes are very rough, which indicates that they are composed of many tiny nanoparticles.

The overall structural features of Co_9S_8 was accessed via XRD experiments (**Figure 2(a)**). The patterns of product are well associated with those of cubic phase Co_9S_8 (JCPDS No. 65-1765). The hollow structure of nanotubes can be confirmed by TEM image (**Figure 2(b)**). High resolution (HRTEM) image (**Figure 2(c)**) shows that the nanotube is composed of tiny nanoparticles with diameters of only several nanometers. The observed interplanar spacing is 0.24 nm and 0.28 nm, which corresponds to the separation between (400) and (222) plane of cubic phase Co_9S_8, respectively. The selected area electron diffraction (SAED) pattern of nanotubes (**Figure 2(d)**) shows distinct diffraction rings, which can be indexed as (311), (511), (440), (533), (642) and (931) lattice planes of cubic phase Co_9S_8.

Chemical states of Co and S were obtained from XPS characterization (**Figure 3**). **Figure 3(a)** shows the core level spectrum of the Co 2p region, with Co $2p_{3/2}$ binding energies at 778.9, 781.2 and 786.5 eV. The peak at 778.9 eV suggests that there are reduced Co species in Co_9S_8 [25]. These reduced Co species are partially charged ($Co^{\delta+}$, $0 < \delta < 2$), and δ must have a small value, because the corresponding Co $2p_{3/2}$ binding energy (778.9 eV) is very close to that of metallic Co (777.9 eV) [21] [26]. In the S 2p spectrum (**Figure 3(b)**), the peak centered at 161.9 eV agrees with the binding energies of Co–S [27] [28].

Figure 4(a) shows the representative polarization data of Co_9S_8/GCE electrodes with different mass loadings, along with the polarization data of a bare GCE and commercial Pt/C catalyst (Johnson Matthey, Hispec 3000, 20 wt%) loaded on GCE. Co_9S_8/GCE electrodes with different loading amounts of Co_9S_8 nanotubes all show apparent current density in the potential range of 0 to −0.4 V vs RHE. The electrocatalytic activity of the Co_9S_8
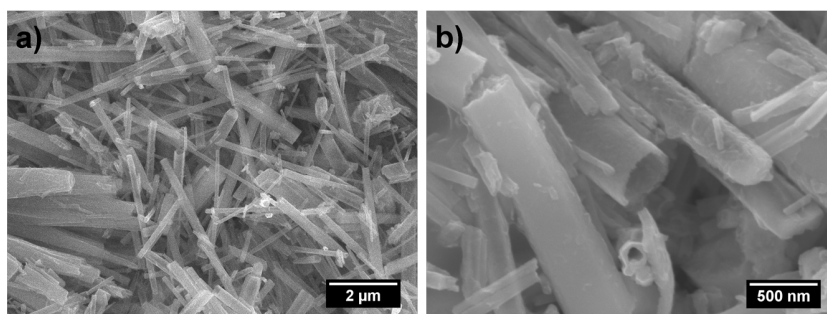
Figure 1. (a) Low and (b) high magnification SEM images of the Co_9S_8 nanotubes.
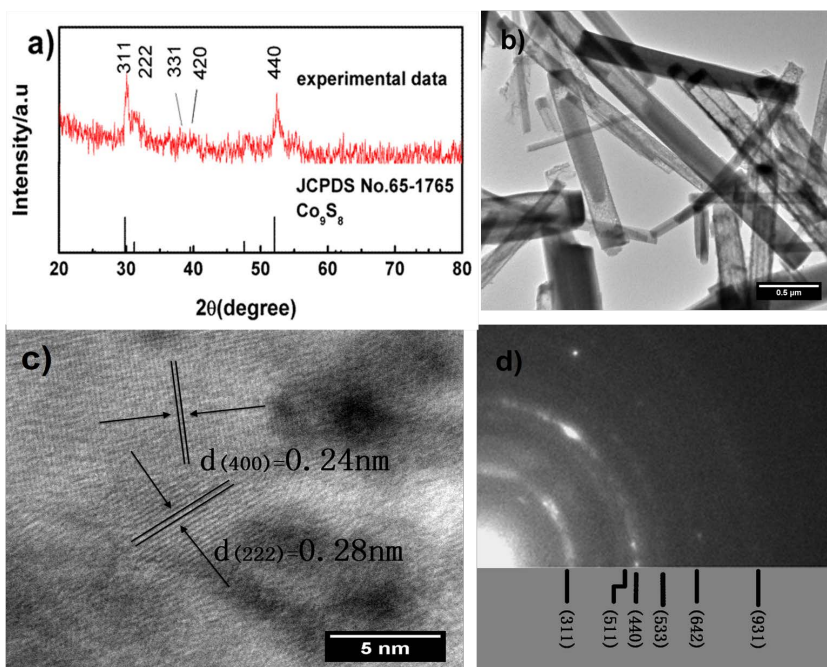
Figure 2. (a) XRD patterns (b) TEM image (c) HRTEM image, and (d) SAED pattern of the Co_9S_8 nanotubes.
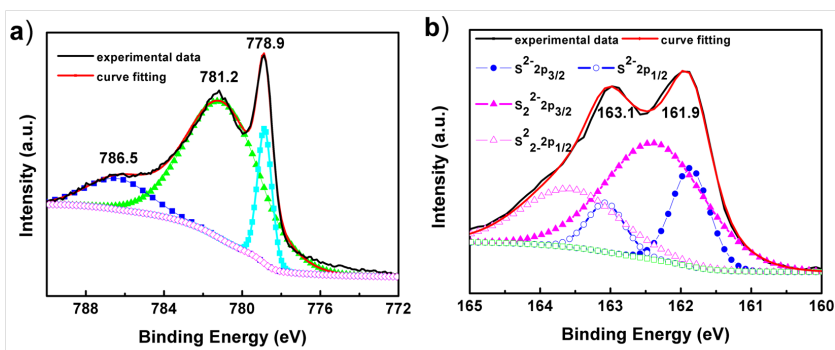
Figure 3. XPS spectra of (a) the Co $2p_{3/2}$ and (b) the S 2p windows of Co_9S_8 sample.

sample is more efficient when the loading amount increased in some degree. The sample with optimal performance (loading amount: 0.855 mg·cm^{-2}) has a current density of 20 mA·cm^{-2} at an overpotential of 320 mV. However, when the loading amount is further increased, the Co_9S_8 doesn't result a better electronic property for

the electrode because it may result in large interface resistance. In contrast, negligible current can be found from the bare GCE electrode, showing that the large current in Co_9S_8/GCE can be definitely correlated with Co_9S_8 nanotubes. The performance of representative HER catalysts is summarized in **Table S1** (Electronic Supplementary Information), which shows that the performance of Co_9S_8 nanotubes is superior to that of Ni_3S_2 loaded on carbon nanotubes and Fe_2P/NGr nanocomposite loaded on GCE.

In a potentiostatic electrolysis experiment, the time-dependent current density recorded from a potentiostatic electrolysis shows only a little degradation in 20,000 s (**Figure 4(b)**). In an accelerated degradation experiment, cyclic voltammetry (CV) sweeps were carried out in the 1 M KOH aqueous solution between −0.380 and 0.100 V *versus* RHE (inset of **Figure 4(b)**). It shows that after continuous cyclic voltammetric (CV) scan for 4000 cycles, the overpotential required for the current density of 20 mA·cm^{-2} (η_{20}) increases from 330 mV to 350 mV. These results suggest Co_9S_8 nanotube can afford long-term hydrogen generation in basic condition.

The faradaic efficiency of Co_9S_8 nanotube in electrolysis of water was evaluated by water-displacement method. **Figure 4(c)** shows the comparison of the theoretical volume of hydrogen and the experimentally measured volume of hydrogen. It is shown that the faradaic yield of H_2 production in a potentiostatic electrolysis of water using Co_9S_8 nanotube as a HER catalyst is nearly 100%.

The Nyquist plots of the Co_9S_8 nanotubes at overpotentials from −200 to −370 mV (**Figure 4(d)**) exhibit classic two time-constant behavior. The semicircles at high frequencies can be related to the contact between the catalyst (Co_9S_8) and the GCE, while those at low frequencies are correlated to the kinetics of the HER process on the surface of the catalyst. The kinetics of electrochemical reaction at an electrode's surface is usually assessed by charge transfer resistance (R_{ct}), with a smaller R_{ct} value corresponding to faster kinetics. R_{ct} was be deduced from EIS spectra by data fitting, in the present case using the equivalent circuit shown in the inset of **Figure 4(d)**. In **Figure 4(e)**, the applied potential is plotted *versus* the inverse R_{ct} on a logarithmic scale, and a Tafel slope was determined to be 135 mV·dec^{-1} according to the slope of linear portion in the plot. The Tafel slope of 135 mV·dec^{-1} suggests that a Volmer-Tafel mechanism is responsible for the HER process on the surface of Co_9S_8 nanotubes.
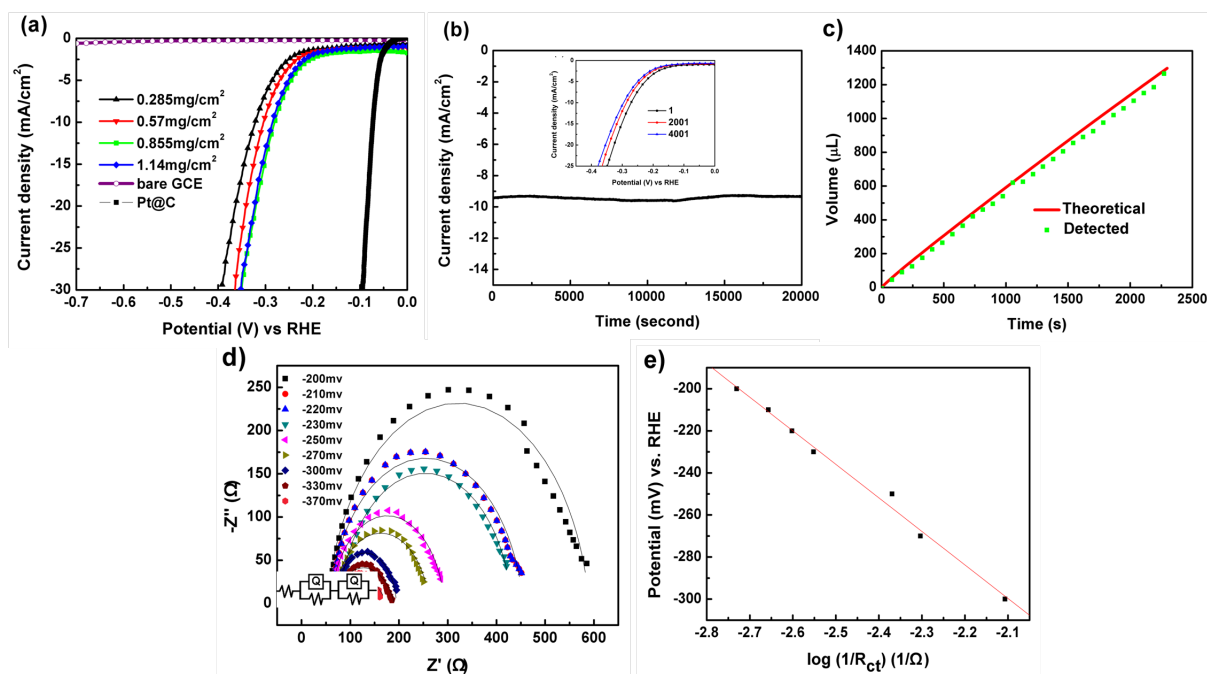
Figure 4. (a) Polarization curves of Co_9S_8 nanotubes and commercial Pt/C catalyst loading on GCE. (b) The time-dependent current density of Co_9S_8 under overpotential of 280 mV for 20,000 s. The inset shows Polarization curves of Co_9S_8 nanotube corresponding to the initial and 4000th CV scans. (c) Current efficiency for H_2 production using Co_9S_8/GCE. (d) Nyquist plots of the Co_9S_8 nanotubes recorded at different overpotentials in 1M KOH. The inset shows the equivalent circuit used for data fitting. (e) Semi-logarithmic plot of applied potential vs log(R_{ct}^{-1}). Only potentials in (a) were corrected with iR drop.

4. Conclusion

In summary, Co_9S_8 nanotubes are found to be an effective HER electrocatalyst. The optimal η_{20} is as small as 320 mV in basic solution. Co_9S_8 nanotubes can work stably in alkaline solutions, and the faradic yield during electrolysis is nearly 100%. The HER process follows a Volmer-Heyrovsky mechanism. The results presented here further demonstrate the promising application potential of metal sulfide in the field of hydrogen generation from electrolysis of water.

Acknowledgements

References

[1]   Turner, J.A. (2004) Sustainable Hydrogen Production. *Science*, **305**, 972-974.
       http://dx.doi.org/10.1126/science.1103197

[2]   Nowotny, J., Sorrell, C.C., Sheppard, L.R. and Bak, T. (2005) Solar-hydrogen: Environmentally safe fuel for the future, *International Journal of Hydrogen Energy*, **30**, 521. http://dx.doi.org/10.1016/j.ijhydene.2004.06.012

[3]   Lin, T.W., Liu, C.J. and Dai, C.S. (2014) Ni_3S_2/Carbon Nanotube Nanocomposite as Electrode Material for Hydrogen Evolution Reaction in Alkaline Electrolyte and Enzyme-Free Glucose Detection. *Applied Catalysis B*: *Environmental*, **154**, 213-220. http://dx.doi.org/10.1016/j.apcatb.2014.02.017

[4]   Li, Y.G., Wang, H.L., Xie, L.M., Liang, Y.Y., Hong, G.S. and Dai, H.J. (2011) MoS_2 Nanoparticles Grown on Graphene: An Advanced Catalyst for the Hydrogen Evolution Reaction. *Journal of the American Chemical Society*, **133**, 7296. http://dx.doi.org/10.1021/ja201269b

[5]   Hinnemann, B., Moses, P.G., Bonde, J., Jorgensen, K.P., Nielsen, J.H., Horch, S., Chorkendorff, I. and Norskov, J.K. (2005) Biornimetic Hydrogen Evolution: MoS_2 Nanoparticles as Catalyst for Hydrogen Evolution. *Journal of the American Chemical Society*, **127**, 5308-5309. http://dx.doi.org/10.1021/ja0504690

[6]   Jaramillo, T.F., Jorgensen, K.P., Bonde, J., Nielsen, J.H., Horch, S. and Chorkendorff, I. (2007) Identification of Active Edge Sites for Electrochemical H_2 Evolution from MoS_2 Nanocatalysts. *Science*, **317**, 100-102. http://dx.doi.org/10.1126/science.1141483

[7]   Lukowski, M.A., Daniel, A.S., Meng, F., Forticaux, A., Li, L.S. and Jin, S. (2013) Enhanced Hydrogen Evolution Catalysis from Chemically Exfoliated Metallic MoS_2 Nanosheets. *Journal of the American Chemical Society*, **135**, 10274. http://dx.doi.org/10.1021/ja404523s

[8]   Voiry, D., Yamaguchi, H., Li, J.W., Silva, R., Alves, D.C.B., Fujita, T., Chen, M.W., Asefa, T., Shenoy, V.B., Eda, G. and Chhowalla, M. (2013) Enhanced Catalytic Activity in Strained Chemically Exfoliated WS_2 Nanosheets for Hydrogen Evolution. *Nature Materials*, **12**, 850. http://dx.doi.org/10.1038/nmat3700

[9]   Huang, Z., Wang, C., Chen, Z., Meng, H., Lv, C., Chen, Z., Han, R. and Zhang, C. (2014) Tungsten Sulfide Enhancing Solar-Driven Hydrogen Production from Silicon Nanowires. *Applied Materials & Interfaces*, **6**, 10408-10414. http://dx.doi.org/10.1021/am501940x

[10]   Faber, M.S., Dziedzic, R., Lukowski, M.A., Kaiser, N.S., Ding, Q. and Jin, S. (2014) High-Performance Electrocatalysis Using Metallic Cobalt Pyrite (CoS_2) Micro- and Nanostructures. *Journal of the American Chemical Society*, **136**, 10053-10061. http://dx.doi.org/10.1021/ja504099w

[11]   Kong, D.S., Wang, H.T., Cha, J.J., Pasta, M., Koski, K.J., Yao, J. and Cui, Y. (2013) Synthesis of MoS_2 and $MoSe_2$ Films with Vertically Aligned Layers. *Nano Letters*, **13**, 1341-1347. http://dx.doi.org/10.1021/nl400258t

[12]   Wang, H.T., Kong, D.S., Johanes, P., Cha, J.J., Zheng, G.Y., Yan, K., Liu, N.A. and Cui, Y. (2013) $MoSe_2$ and WSe_2 Nanofilms with Vertically Aligned Molecular Layers on Curved and Rough Surfaces. *Nano Letters*, **13**, 3426-3433. http://dx.doi.org/10.1021/nl401944f

[13]   Kong, D.S., Wang, H.T., Lu, Z.Y. and Cui, Y. (2014) $CoSe_2$ Nanoparticles Grown on Carbon Fiber Paper: An Efficient and Stable Electrocatalyst for Hydrogen Evolution Reaction. *Journal of the American Chemical Society*, **136**, 4897-4900. http://dx.doi.org/10.1021/ja501497n

[14]   Vrubel, H. and Hu, X.L. (2012) Molybdenum Boride and Carbide Catalyze Hydrogen Evolution in both Acidic and Basic Solutions. *Angewandte Chemie International Edition*, **51**, 12703-12706. http://dx.doi.org/10.1002/anie.201207111

[15] Chen, W.F., Wang, C.H., Sasaki, K., Marinkovic, N., Xu, W., Muckerman, J.T., Zhu, Y. and Adzic, R.R. (2013) Highly Active and Durable Nanostructured Molybdenum Carbide Electrocatalysts for Hydrogen Production. *Energy & Environmental Science*, **6**, 943-951. http://dx.doi.org/10.1039/c2ee23891h

[16] Chen, W.F., Sasaki, K., Ma, C., Frenkel, A.I., Marinkovic, N., Muckerman, J.T., Zhu, Y.M. and Adzic, R.R. (2012) Hydrogen-Evolution Catalysts Based on Non-Noble Metal Nickel-Molybdenum Nitride Nanosheets. *Angewandte Chemie International Edition*, **51**, 6131-6135. http://dx.doi.org/10.1002/anie.201200699

[17] Cao, B.F., Veith, G.M., Neuefeind, J.C., Adzic, R.R. and Khalifah, P.G. (2013) Mixed Close-Packed Cobalt Molybdenum Nitrides as Non-Noble Metal Electrocatalysts for the Hydrogen Evolution Reaction. *Journal of the American Chemical Society*, **135**, 19186-19192. http://dx.doi.org/10.1021/ja4081056

[18] Xiao, P., Sk, M.A., Thia, L., Ge, X., Lim, R.J., Wang, J.Y., Lim, K.H. and Wang, X. (2014) Molybdenum Phosphide as an Efficient Electrocatalyst for Hydrogen Evolution Reaction. *Energy & Environmental Science*, **7**, 2624-2629. http://dx.doi.org/10.1039/C4EE00957F

[19] Popczun, E.J., McKone, J.R., Read, C.G., Biacchi, A.J., Wiltrout, A.M., Lewis, N.S. and Schaak, R.E. (2013) Nanostructured Nickel Phosphide as an Electrocatalyst for the Hydrogen Evolution Reaction. *Journal of the American Chemical Society*, **135**, 9267-9270. http://dx.doi.org/10.1021/ja403440e

[20] Huang, Z., Chen, Z., Chen, Z., Lv, C., Meng, H. and Zhang, C. (2014) $Ni_{12}P_5$ Nanoparticles as an Efficient Catalyst for Hydrogen Generation via Electrolysis and Photoelectrolysis. *ACS NANO*, **8**, 8121-8129. http://dx.doi.org/10.1021/nn5022204

[21] Huang, Z., Chen, Z., Chen, Z., Lv, C., G.Humphrey, M. and Zhang, C. (2014) Cobalt Phosphide Nanorods as an Efficient Electrocatalyst for the Hydrogen Evolution Reaction. *Nano Energy*, **9**, 373-382. http://dx.doi.org/10.1016/j.nanoen.2014.08.013

[22] Popczun, E.J., Read, C.G., Roske, C.W., Lewis, N.S. and Schaak, R.E. (2014) Highly Active Electrocatalysis of the Hydrogen Evolution Reaction by Cobalt Phosphide Nanoparticles. *Angewandte Chemie International Edition*, **53**, 5427-5430. http://dx.doi.org/10.1002/anie.201402646

[23] Wang, Z.H., Chen, X.Y., Zhang, M. and Qian, Y.T. (2005) Synthesis of Co_3O_4 Nanorod Bunches from a Single Precursor $Co(CO_3)_{(0.35)}Cl_{0.20}(OH)_{(1.10)}$. *Solid State Sciences*, **7**, 13-15. http://dx.doi.org/10.1016/j.solidstatesciences.2004.10.032

[24] Wang, Z.H., Pan, L., Hu, H.B. and Zhao, S.P. (2010) Co_9S_8 Nanotubes Synthesized on the Basis of Nanoscale Kirkendall Effect and Their Magnetic and Electrochemical Properties. *CrystEngComm*, **12**, 1899-1904. http://dx.doi.org/10.1039/b923206k

[25] Yan, Y., Ge, X., Liu, Z., Wang, J.-Y., Leea, J.-M. and Wang, X. (2013) Facile Synthesis of Low Crystalline MoS_2 Nanosheet-Coated CNTs for Enhanced Hydrogen Evolution Reaction. *Nanoscale*, **5**, 7768-7771. http://dx.doi.org/10.1039/c3nr02994h

[26] Nemoshalenko, V.V., Didyk, V.V., Krivitskii, V.P. and Senekevich, A.I. (1983) Investigation of the Atomic Charges in Iron, Cobalt and Nickel Phosphides. *Zhurnal Neorganicheskoi Khimii*, **28**, 2182.

[27] Pu, J., Wang, Z., Wu, K., Yu, N. and Sheng, E. (2014) Co_9S_8 Nanotube Arrays Supported on Nickel Foam for High-Performance Supercapacitors. *Physical Chemistry Chemical Physics*, **16**, 785-791. http://dx.doi.org/10.1039/C3CP54192D

[28] Bao, S.J., Li, Y., Li, C.M., Bao, Q., Lu, Q. and Guo, J. (2008) Shape Evolution and Magnetic Properties of Cobalt Sulfide. *Crystal Growth & Design*, **8**, 3745-3749. http://dx.doi.org/10.1021/cg800381e

Supplement: Electronic Supporting Information

S1. Experimental

S1.1. Materials Synthesis

The method used in the synthesis of $Co(CO_3)_{0.35}Cl_{0.20}(OH)_{1.10}$ nanorods was adopted from those reported in ref [1] [2]. Then, 0.6 mmol of the as-prepared $Co(CO_3)_{0.35}Cl_{0.20}(OH)_{1.10}$ and 0.629 mL of a supersaturated Na_2S aqueous solution were loaded into a Teflon liner (40 mL) with 30 ml distilled water [2]. The liner was sealed in a stainless steel autoclave and maintained at 160˚C for 8 h, then cooled naturally to room temperature. The black precipitates were filtered off, washed with distilled water and ethanol, and then dried at 60˚C.

S1.2. Material Characterization

The morphologies were accessed by scanning electron microscopy (SEM, 7001F, JEOL) and transmission electron microscopy (TEM, 2100, JEOL). The X-ray photoelectron spectroscopy (XPS) experiments were carried out on a Physical Electronics PHI 5700 ESCA System. Powder X-ray diffraction (XRD) patterns were collected with a D8 ADVANCE.

The electrochemical measurements were carried out in an aqueous 1M KOH solution with an electrochemical workstation (CHI614D, CH Instrument). A three-electrode configuration was adopted in the measurements, with Co_9S_8 loading on GCE as the working electrode, a graphite rodas the counter electrode and a Mercury/Mercury Oxide electrode (MOE, Hg/HgO) as the reference electrode. The reversible hydrogen evolution potential (RHE) was determined to be −0.879 V vs MOE by the open circuit potential of a clean Pt electrode in the same solution. For the evaluation of HER catalytic activity, Co_9S_8 nanotubes (4 mg) were dispersed in 1 mL of water/ethanol (4/1, V/V) containing 80 μL of Nafion solution (5 wt%). The evaluation of the HER catalytic activity of Co_9S_8 loaded on GCE was carried out by linear sweep voltammetry (5 mV·s^{-1}). The volume of H_2 during potentiostatic electrolysis measurement was monitored by volume displacement in a configuration as shown in ref [3].

Table S1. Summary of the HER performance of representative catalysts.

Catalyst	Substrate	Mass density (mg/cm^2)	η_{onset} (mV)	η_{10} (mV)	η_{20} (mV)	Tafel slope (mV/dec)	Electrolyt
Ni-Mo nanopowder [4]	Ti foil	1	-	79	107	-	1M NaOH
Co$_2$P [3]	Ti foil	1	100	150	171	58	1 M KOH
Ni$_2$P [5]	Ti foil	1	50	174	205	95	1 M KOH
CoP/CC [6]	Carbon cloth	0.92	140	203	245	129	1 M KOH
Ni/MWCNT [7]	-	-		180	220	102	1 M KOH
Ni$_3$S$_2$/MWCNT-NC) [8]	-	-	400	490	510	167	1 M KOH
Ni$_3$S$_2$/MWCNT-NC (333K) [8]	-	-	300	330	375	202	1 M KOH
KOH-treated Ni$_3$S$_2$/MWCNT-NC (298K) [8]	-	-	200	340	400	102	1 M KOH
KOH-treated Ni$_3$S$_2$/MWCNT-NC (323K) [8]	-	-	150	210	270	109	1 M KOH
Ni$_3$S$_2$ (298K) [8]	-	-	420	>500	>500	101	1 M KOH
Ni$_3$S$_2$ (333K) [8]	-	-	250	370	400	203	1 M KOH
MoB [9]	carbon-paste electrode	2.3	120	220	240	59	1 M KOH
Mo$_2$C [9]	carbon-paste electrode	0.8	120	190	210	54	1 M KOH
Fe$_2$P/NGr [10]	GCE	1.71	210	355	376	-	1 M KOH
MoS2/RGO [11]	GCE	0.28	90	155	180	41	0.5 M H$_2$SO$_4$
MoS$_2$ Nanosheets [12]	Graphite	-	150	187	200	43	0.5 M H$_2$SO$_4$

Continued

WS_2 [13]	GCE	0.285	500	750	800	-	0.05 M H_2SO_4
WS_3 [13]	GCE	0.285	500	670	710	-	0.05 M H_2SO_4
CoS_2 nanowire [14]	rotating disk electrode	1.7	75	145	160	51.6	0.5 M H_2SO_4
CoS_2 microwire [14]	rotating disk electrode	25	75	158	175	58	0.5 M H_2SO_4
$MoSe_2$ film [15]	GCE	-	160	-	-	106	0.5 M H_2SO_4
WSe_2 film [16]	Carbon fiber paper	-	150	300	-	77.4	0.5 M H_2SO_4
$CoSe_2$ nanoparticles [17]	Carbon fiber paper	-	80	137	150	42.1	0.5 M H_2SO_4
MoB [18]	disk electrode	2.5	120	211	227	55	1 M H_2SO_4
Mo_2C/CNT [19]	-	-	63	150	-	55.2	0.1 M $HClO_4$
Mo_2C/XC [19]	-	-	105	-	-	59.4	0.1 M $HClO_4$
$NiMoN_x$/C [20]	-	-	78	-	-	35.9	0.1 M $HClO_4$
$Co_{0.6}Mo_{1.4}N_2$ [21]	rotating disk electrode	0.24	-	200	270	-	0.1 M $HClO_4$
MoP [22]	GCE	-	50	140	160	54	0.5 M H_2SO_4
CoP [23]	To foil	2	-	75	85	50	0.5 M H_2SO_4
Co_9S_8 (this work)	GCE	0.855	200	280	320	135	1 M KOH

References

[1] Wang, Z.H., Chen, X.Y., Zhang, M. and Qian, Y.T. (2005) Synthesis of Co_3O_4 Nanorod Bunches from a Single Precursor $Co(CO_3)_{(0.35)}Cl_{0.20}(OH)_{(1.10)}$. *Solid State Sciences*, **7**, 13-15. http://dx.doi.org/10.1016/j.solidstatesciences.2004.10.032

[2] Wang, Z.H., Pan, L., Hu, H.B. and Zhao, S.P. (2010) Co_9S_8 Nanotubes Synthesized on the Basis of Nanoscale Kirkendall Effect and Their Magnetic and Electrochemical Properties. *CrystEngComm*, **12**, 1899-1904. http://dx.doi.org/10.1039/b923206k

[3] Huang, Z., Chen, Z., Chen, Z., Lv, C., Humphrey, M.G. and Zhang, C. (2014) Cobalt Phosphide Nanorods as an Efficient Electrocatalyst for the Hydrogen Evolution Reaction. *Nano Energy*, **9**, 373-382. http://dx.doi.org/10.1016/j.nanoen.2014.08.013

[4] McKone, J.R., Sadtler, B.F., Werlang, C.A., Lewis, N.S. and Gray, H.B. (2013) Ni-Mo Nanopowders for Efficient Electrochemical Hydrogen Evolution. *ACS Catalysis*, **3**, 166-169. http://dx.doi.org/10.1021/cs300691m

[5] Popczun, E.J., McKone, J.R., Read, C.G., Biacchi, A.J., Wiltrout, A.M., Lewis, N.S. and Schaak, R.E. (2013) Nanostructured Nickel Phosphide as an Electrocatalyst for the Hydrogen Evolution Reaction. *Journal of the American Chemical Society*, **135**, 9267-9270. http://dx.doi.org/10.1021/ja403440e

[6] Tian, J., Liu, Q., Asiri, A.M. and Sun, X. (2014) Self-Supported Nanoporous Cobalt Phosphide Nanowire Arrays: An Efficient 3D Hydrogen-Evolving Cathode over the Wide Range of pH 0-14. *Journal of the American Chemical Society*, **136**, 7587-7590. http://dx.doi.org/10.1021/ja503372r

[7] McArthur, M.A., Jorge, L., Coulombe, S. and Omanovic, S. (2014) Synthesis and Characterization of 3D Ni Nanoparticle/Carbon Nanotbe Cathodes for Hydrogen Evolution in Alkaline Electrolyte. *Journal of Power Sources*, **266**, 365-373. http://dx.doi.org/10.1016/j.jpowsour.2014.05.036

[8] Lin, T.W., Liu, C.J. and Dai, C.S. (2014) Ni_3S_2/Carbon Nanotube Nanocomposite as Electrode Material for Hydrogen Evolution Reaction in Alkaline Electrolyte and Enzyme-Free Glucose Detection. *Applied Catalysis B*: *Environmental*, **154**, 213-220. http://dx.doi.org/10.1016/j.apcatb.2014.02.017

[9] Vrubel, H. and Hu, X.L. (2012) Molybdenum Boride and Carbide Catalyze Hydrogen Evolution in both Acidic and Basic Solutions. *Angewandte Chemie International Edition*, **51**, 12703-12706. http://dx.doi.org/10.1002/anie.201207111

[10] Huang, Z., Lv, C., Chen, Z., Chen, Z., Tian, F. and Zhang, C. (2015) One-Pot Synthesis of Diiron Phosphide/Nitrgen-Doped Graphene Nanocomposite for Effective Hydrogen Generation. *Nano Energy*, **12**, 666-674. http://dx.doi.org/10.1016/j.nanoen.2015.01.027

[11] Li, Y.G., Wang, H.L., Xie, L.M., Liang, Y.Y., Hong, G.S. and Dai, H.J. (2011) MoS$_2$ Nanoparticles Grown on Graphene: An Advanced Catalyst for the Hydrogen Evolution Reaction. *Journal of the American Chemical Society*, **133**, 7296-7299. http://dx.doi.org/10.1021/ja201269b

[12] Lukowski, M.A., Daniel, A.S., Meng, F., Forticaux, A., Li, L.S. and Jin, S. (2013) Enhanced Hydrogen Evolution Catalysis from Chemically Exfoliated Metallic MoS$_2$ Nanosheets. *Journal of the American Chemical Society*, **135**, 10274-10277. http://dx.doi.org/10.1021/ja404523s

[13] Huang, Z., Wang, C., Chen, Z., Meng, H., Lv, C., Chen, Z., Han, R. and Zhang, C. (2014) Tungsten Sulfide Enhancing Solar-Driven Hydrogen Production from Silicon Nanowires. *ACS Applied Materials & Interfaces*, **6**, 10408-10414. http://dx.doi.org/10.1021/am501940x

[14] Faber, M.S., Dziedzic, R., Lukowski, M.A., Kaiser, N.S., Ding, Q. and Jin, S. (2014) High-Performance Electrocatalysis Using Metallic Cobalt Pyrite (CoS$_2$) Micro- and Nanostructures. *Journal of the American Chemical Society*, **136**, 10053-10061. http://dx.doi.org/10.1021/am501940x

[15] Kong, D.S., Wang, H.T., Cha, J.J., Pasta, M., Koski, K.J., Yao, J. and Cui, Y. (2013) Synthesis of MoS$_2$ and MoSe$_2$ Films with Vertically Aligned Layers. *Nano Letters*, **13**, 1341-1347. http://dx.doi.org/10.1021/nl400258t

[16] Wang, H.T., Kong, D.S., Johanes, P., Cha, J.J., Zheng, G.Y., Yan, K., Liu, N.A. and Cui, Y. (2013) MoSe$_2$ and WSe$_2$ Nanofilms with Vertically Aligned Molecular Layers on Curved and Rough Surfaces. *Nano Letters*, **13**, 3426-3433. http://dx.doi.org/10.1021/nl401944f

[17] Kong, D.S., Wang, H.T., Lu, Z.Y. and Cui, Y. (2014) CoSe$_2$ Nanoparticles Grown on Carbon Fiber Paper: An Efficient and Stable Electrocatalyst for Hydrogen Evolution Reaction. *Journal of the American Chemical Society*, **136**, 4897-4900. http://dx.doi.org/10.1021/ja501497n

[18] Vrubel, H. and Hu, X.L. (2012) Molybdenum Boride and Carbide Catalyze Hydrogen Evolution in both Acidic and Basic Solutions. *Angewandte Chemie International Edition*, **51**, 12703-12706. http://dx.doi.org/10.1002/anie.201207111

[19] Chen, W.F., Wang, C.H., Sasaki, K., Marinkovic, N., Xu, W., Muckerman, J.T., Zhu, Y. and Adzic, R.R. (2013) Highly Active and Durable Nanostructured Molybdenum Carbide Electrocatalysts for Hydrogen Production. *Energy & Environmental Science*, **6**, 943-951. http://dx.doi.org/10.1039/c2ee23891h

[20] Chen, W.F., Sasaki, K., Ma, C., Frenkel, A.I., Marinkovic, N., Muckerman, J.T., Zhu, Y.M. and Adzic, R.R. (2012) Hydrogen-Evolution Catalysts Based on Non-Noble Metal Nickel-Molybdenum Nitride Nanosheets. *Angewandte Chemie International Edition*, **51**, 6131-6135. http://dx.doi.org/10.1002/anie.201200699

[21] Cao, B.F., Veith, G.M., Neuefeind, J.C., Adzic, R.R. and Khalifah, P.G. (2013) Mixed Close-Packed Cobalt Molybdenum Nitrides as Non-Noble Metal Electrocatalysts for the Hydrogen Evolution Reaction. *Journal of the American Chemical Society*, **135**, 19186-19192. http://dx.doi.org/10.1021/ja4081056

[22] Xiao, P., Sk, M.A., Thia, L., Ge, X., Lim, R.J., Wang, J.Y., Lim, K.H. and Wang, X. (2014) Molybdenum Phosphide as an Efficient Electrocatalyst for Hydrogen Evolution Reaction. *Energy & Environmental Science*, **7**, 2624-2629. http://dx.doi.org/10.1039/C4EE00957F

[23] Popczun, E.J., Read, C.G., Roske, C.W., Lewis, N.S. and Schaak, R.E. (2014) Highly Active Electrocatalysis of the Hydrogen Evolution Reaction by Cobalt Phosphide Nanoparticles. *Angewandte Chemie International Edition*, **53**, 5427-5430. http://dx.doi.org/10.1002/anie.201402646